AIAA 80-0314R

Thermal Convection in an Enclosure Due to Vibrations Aboard Spacecraft

Y. Kamotani,* A. Prasad,† and S. Ostrach‡
Case Western Reserve University, Cleveland, Ohio

This paper discusses thermal convection in an enclosure induced by spacecraft vibrations (*g*-jitter). Under normal circumstances (no maneuvers, no intentional spinning of the spacecraft) the *g*-jitter generates predominantly oscillatory velocity and temperature fields with zero time-mean values. The *g*-jitter can also generate secondary flows with nonzero mean, but they are of much smaller order. Some implications of the *g*-jitter on materials processing in space are discussed.

Introduction

ONE of the primary advantages foreseen for processing of materials in space is the reduction of natural convection associated with the Earth's gravity. However, there have been some indications (e.g., Apollo 14 experiments[1,2]) that spacecraft vibrations might cause appreciable thermal convection. Such convection may be important in fluids experiments and also affect the quality of crystals grown in space. Therefore, to study the effectiveness of spacecraft vibrations in generating fluid flows, the present work theoretically investigates a case in which a fluid-filled container with differentially heated walls is subjected to spacecraft vibrations. Implications of the results for space processing are discussed.

In an attempt to evaluate the effects of *g*-jitter on fluid motions Spradley el al.[3] made a numerical analysis for various configurations. They considered three *g*-jitter profiles, sinusoidal, absolute sinusoidal and saw tooth, and compared the flowfields with that for constant *g* level. They found that if the *g*-jitter is decomposed into a time mean part and an oscillatory part, the mean part is more important than the oscillatory part in determining the flowfield and heat-transfer rate. A somewhat related work has been done by Forbes[4] where the effect of sinusoidal vibrations on natural convective heat transfer in a rectangular enclosure is studied experimentally as well as numerically under 1-*g* conditions. The results indicate that the vibrations have very little effect on the heat transfer when the flow is laminar.

The present study is more comprehensive than the work by Spradley et al.,[3] and is meant to give a better physical insight into the *g*-jitter in space. Some of the material presented herein is taken from the work by Prasad and Ostrach.[5]

Formulation of the Problem

g-Jitter

Consider an experimental setup which is in a spaceship orbiting the Earth (Fig. 1). The coordinates (X_0, Y_o, Z_0) are fixed at the center of the Earth with origin 0 (fixed frame of reference), and the coordinates (X', Y', Z') are attached to the spacecraft with origin 0′ at its center of mass. The coordinates (x,y,z) are attached to the experiment. We suppose that the coordinates (X', Y', Z') are rotating with angular velocity Ω about the origin 0′. Then the absolute acceleration of a moving fluid element in the experiment is given by

$$a=\frac{Du}{Dt}+2\Omega\times u+\frac{d\Omega}{dt}\times(R'+r)$$
$$+\Omega\times(\Omega\times(R'+r))+g+a_0+F/M \qquad (1)$$

where u and r are the velocity and location, respectively, of the element with respect to (x,y,z), a_0 is the acceleration of 0′ with respect to (X_0, Y_0, Z_0) caused by centrifugal and aerodynamic forces on the spacecraft, g is the gravitational acceleration which acts toward 0, and F denotes forces applied to the spacecraft whose mass is M.

When u, Ω, and F are zero, then the force per unit mass acting on the fluid element is given as

$$\Delta g=g+a_0$$

where $|\Delta g|$ is called the reduced-gravity level whose value varies depending on the position in the spacecraft. Because of such variation of Δg inside the spacecraft, the spacecraft generally spins slowly around its center of mass, and thruster engines are used to correct its attitude. Other possible sources of external forces are crew motions and onboard machine vibrations. When forces act on the spacecraft, the moving fluid element experiences a body force per unit mass according to Eq. (1)

$$f=2\Omega\times u+\frac{d\Omega}{dt}\times(R'+r)$$
$$+\Omega\times(\Omega\times(R'+r))+g+a_0+F/M \qquad (2)$$

in addition to the real acceleration Du/Dt in the moving frame. $|f|$ is termed *g*-jitter level.

For the spacecraft to remain in orbit (no maneuvers) it is necessary that the time-average of the forces F must vanish. In the present study the situation in which the spacecraft is intentionally spinning is not considered so that the time-average of Ω is also taken to be zero herein. The third term on the right-hand side of Eq. (2) represents the centrifugal force due to spacecraft oscillations and it has been shown in Ref. 6 to be negligible under normal circumstances.

In view of all the above contributions to the body force, Eq. (2), except for the reduced gravity terms must be of an oscillatory nature. Since the reduced gravity level is usually between 10^{-7} to 10^{-9} g_0, where g_0 is the gravitational acceleration on the surface of the Earth, and at any instant of

Presented as Paper 80-0314 at the AIAA 18th Aerospace Sciences Meeting, Pasadena, Calif., Jan. 14-16, 1980; submitted Jan. 16, 1980; revision received Oct. 22, 1980.

*Associate Professor, Dept. of Mechanical and Aerospace Engineering. Member AIAA.

†Graduate Student; presently, Research Engineer, Midland-Ross Corp., Toledo, Ohio.

‡Professor, Dept. of Mechanical and Aerospace Engineering. Fellow AIAA.

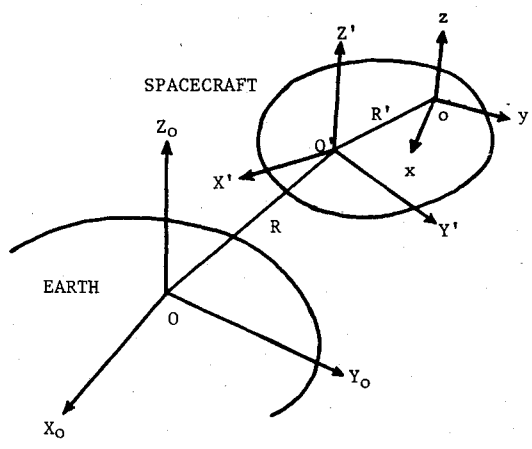

Fig. 1 Coordinate systems.

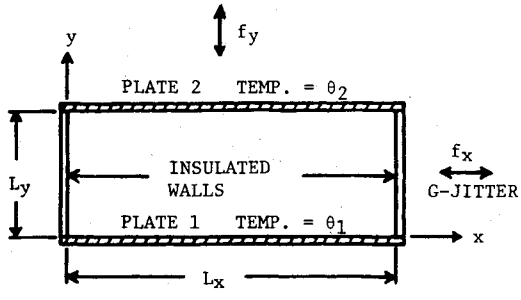

Fig. 2 Experiment—fixed coordinate system.

time the oscillatory part of the g-jitter can be as great as 10^{-3} g_0 (Ref. 2), the latter contributes most to the g-jitter. In reality the g-jitter vector f changes randomly with time. However, in the present work the g-jitter level is simulated by a sinusoidal function of time superposed on a constant reduced gravity level.

Basic Equations

Consider a rectangular container filled with fluid (Fig. 2). Plate 1 is maintained at temperature θ_1, and plate 2 at θ_2, and the other walls are thermally insulated. The basic equations with respect to the coordinate system (x,y,z) are as follows.

Continuity equation:

$$\frac{\partial \rho}{\partial t} + \nabla \cdot (\rho u) = 0 \tag{3}$$

Momentum equation:

$$\rho \frac{Du}{Dt} = -\nabla p + \mu \nabla^2 u + \frac{\mu}{3} \nabla (\nabla \cdot u) - \rho f \tag{4}$$

Energy equation:

$$\rho C_p \frac{D\theta}{Dt} = k \nabla^2 \theta \tag{5}$$

In general the body force due to g-jitter can act in any direction. However, at first, it is assumed that the g-jitter acts only in the x direction, normal to the imposed temperature gradient, and thus the flow is considered to be uniform in the z direction (two-dimensional flow). We consider the g-jitter which is expressed as

$$f_x = A' F(t) + F_m, \quad f_y = f_z = 0$$

where A' is the amplitude of the oscillatory part and F_m is the mean g-jitter level. If the oscillatory part is caused by a periodic vibration of amplitude a and frequency ω, then $A' = a\omega^2$.

The boundary conditions are the no-slip conditions on the wall surfaces for velocities and specified temperatures at plates 1 and 2 and insulated conditions on the other walls.

Equations (3-5) are nondimensionalized by introducing the following:

$$X = x/L_x, \quad Y = y/L_y, \quad \tau = \omega t, \quad U = u/a\omega,$$

$$V = (v/a\omega)L_x/L_y, \quad P = (p/\rho(a\omega)^2)a/L_x,$$

$$T = (\theta - \theta_1)/(\theta_2 - \theta_1) = (\theta - \theta_1)/\Delta T$$

The characteristic velocity $a\omega$ in the x direction is obtained by equating the dominant body force term and the unsteady term in the x-direction momentum equation, since those are two dominant terms in the equation as long as the Reynolds number is much larger than unity as shown below.

If the pressure in the container is constant (by means of bleed openings), variation of density with temperature is expressed as

$$\rho = \rho_r(1 - \beta(\theta - \theta_r)) = \rho_r(1 - \beta\Delta T(T - T_r)) \tag{6}$$

where θ_r is a reference temperature. The coefficient of volumetric expansion β is, in general, on the order of 10^{-2}-10^{-4} (1/°C), and thus $\beta\Delta T$ is considered to be small. As in natural convection problems,[7] the dependent variables in Eqs. (3-5) are expanded in terms of $\epsilon = \beta\Delta T$, namely

$$U = U_0 + \epsilon U_1 \tag{7a}$$

$$V = V_0 + \epsilon V_1 \tag{7b}$$

$$T = T_0 + \epsilon(a/L_x) T_1 \tag{7c}$$

$$P = P_0 + \epsilon P_1 \tag{7d}$$

Substitution of Eq. (7) into Eqs. (3-5), followed by the formal process of equating terms of like power in ϵ, yields a set of differential equations for each power in ϵ.

It can be shown[5] that the zeroth order solution is simply a hydrostatic balance, namely $U_0 = V_0 = 0$. This means that the whole fluid moves as a bulk with the container to this order of approximation. The fact that there is no fluid motion in this order of approximation was shown in the drop-tower tests reported by Prasad and Ostrach.[5] The zeroth-order temperature distribution is described by conduction,

$$\frac{\partial T_0}{\partial \tau} = \frac{\nu}{\omega L_x^2} \frac{1}{Pr} \left[\frac{\partial^2 T_0}{\partial X^2} + \left(\frac{L_x}{L_y} \right)^2 \frac{\partial^2 T_0}{\partial Y^2} \right] \tag{8}$$

where Pr is the Prandtl number. Under steady conditions T_0 is simply expressed as $T_0 = Y$.

Therefore, as in natural convection problems, the most important equations are on the order of ϵ. The first-order equations are as follows:

$$\frac{\partial U_1}{\partial X} + \frac{\partial V_1}{\partial Y} = 0 \tag{9}$$

$$\frac{DU_1}{D\tau} = -\frac{\partial P_1}{\partial X} + \frac{\nu}{\omega L_x^2} \nabla^2 U_1 + \left(T_0 + \epsilon \frac{a}{L_x} T_1 \right) \left(F(\tau) + \frac{F_m}{a\omega^2} \right) \tag{10}$$

$$\frac{DV_1}{D\tau} = -\left(\frac{L_x}{L_y} \right)^2 \frac{\partial P_1}{\partial Y} + \frac{\nu}{\omega L_x^2} \nabla^2 V_1 \tag{11}$$

$$\frac{DT_1}{D\tau} = \frac{\nu}{\omega L_{x^2}} \frac{1}{Pr} \nabla^2 T_1 - V_1 \frac{\partial T_0}{\partial Y} \tag{12}$$

where $D/D\tau = \partial/\partial\tau + \epsilon a/L_x (U_1 \partial/\partial X + V_1 \partial/\partial Y)$ and $\nabla^2 = \partial^2/\partial X^2 + (L_x/L_y)^2 \partial^2/\partial Y^2$.

The boundary and initial conditions are;

$$U_1(X,0,\tau) = U_1(X,1,\tau) = U_1(0,Y,\tau) = U_1(1,Y,\tau) = 0$$

$$V_1(X,0,\tau) = V_1(X,1,\tau) = V_1(0,Y,\tau) = V_1(1,Y,\tau) = 0$$

$$T_1(X,0,\tau) = T_1(X,1,\tau) = 0$$

$$\partial T_1(0,Y,\tau)/\partial X = \partial T_1(1,Y,\tau)/\partial X = 0$$

$$U_1(X,Y,0) = V_1(X,Y,0) = T_1(X,Y,0) = 0$$

The following significant dimensionless parameters in the problem appear in Eqs. (10-12): $\omega L_{x^2}/\nu = Re$ = Reynolds number, ratio of viscous diffusion time to period of oscillation; Pr = Prandtl number; $L_x/L_y = Ar$ = aspect ratio; $\epsilon a/L_x = \epsilon A$ = relative amplitude of fluid oscillation; and $F_m/a\omega^2$ = ratio of mean g-jitter level to oscillatory level.

The values of Pr for liquid metals are on the order of 10^{-2}, and for water Pr is about 10. This is the range of Pr studied herein. In space flight ω is typically 0.1-10 rad/s (Ref. 6) and the values of ν for liquids, gases, and liquid metals are on the order of 10^{-5}-10^{-7} m^2/s. Therefore Re is considered to be larger than unity unless one has a very small scale setup ($L_x, L_y < 1$ cm). The aspect ratio is considered to be unity in the following analysis, but other aspect ratios are also studied in some cases. The present analysis deals mainly with predominantly oscillatory disturbances which persist more than 3 to 4 cycles. Such disturbances are caused by crew motions, intermittent thruster firings for attitude control and on-board machine vibrations. Typically $a\omega^2$ is on the order 10^{-3}-10^{-5} g_0 and F_m 10^{-7}-10^{-9} g_0. Therefore the ratio $F_m/a\omega^2$ is typically less than 10^{-2}. The parameter ϵA is considered to much smaller than unity. When $A\,(=a/L_x) < 1$, then $\epsilon A < \epsilon$ so that the terms of order ϵA in Eqs. (10-12) are at most one order of magnitude smaller than other terms, and thus those terms are considered to be negligible in the present analysis. On the other hand when $A > 1$, then $\epsilon < \epsilon A \ll 1$ so that the terms of order ϵA are retained as correction terms.

Analysis

Steady-State Analysis

Steady-state solutions are studied first. It is convenient to decompose the velocities, temperature and pressure into the oscillatory parts and the mean parts as follows:

$$U_1 = U_1' + \epsilon A \bar{U}_1 \tag{13a}$$

$$V_1 = V_1' + \epsilon A \bar{V}_1 \tag{13b}$$

$$T_1 = T_1' + \epsilon A \bar{T}_1 \tag{13c}$$

$$P_1 = P_1' + \epsilon A \bar{P}_1 \tag{13d}$$

The overbar denotes time averages. The equations for the fluctuating and mean flowfields are obtained by substituting Eq. (13) into Eqs. (9-12), and following the procedures used to study turbulent flows. The following equations are obtained by noting that under steady-state conditions $T_0 = Y$, and neglecting small order terms.

For the fluctuating flowfield,

$$\frac{\partial U_1'}{\partial X} + \frac{\partial V_1'}{\partial Y} = 0 \tag{14}$$

$$\frac{\partial U_1'}{\partial \tau} = -\frac{\partial P_1'}{\partial X} + \frac{1}{Re} \nabla^2 U_1' + YF(\tau) \tag{15}$$

$$\frac{\partial V_1'}{\partial \tau} = -A_r^2 \frac{\partial P_1'}{\partial Y} + \frac{1}{Re} \nabla^2 V_1' \tag{16}$$

$$\frac{\partial T_1'}{\partial \tau} = \frac{1}{Pe} \nabla^2 T_1' - V_1' \tag{17}$$

where $Pe = RePr$.

For the mean flowfield.

$$\frac{\partial \bar{U}_1}{\partial X} + \frac{\partial \bar{V}_1}{\partial Y} = 0 \tag{18}$$

$$\frac{1}{Re} \nabla^2 \bar{U}_1 - \frac{\partial \bar{P}_1}{\partial X} = \overline{U_1' \frac{\partial U_1'}{\partial X}} + \overline{V_1' \frac{\partial U_1'}{\partial Y}} - \overline{T_1' F(\tau)} - \frac{1}{\epsilon A} \frac{F_m}{a\omega^2} \tag{19}$$

$$\frac{1}{Re} \nabla^2 \bar{V}_1 - A_r^2 \frac{\partial \bar{P}_1}{\partial Y} = \overline{U_1' \frac{\partial V_1'}{\partial X}} + \overline{V_1' \frac{\partial V_1'}{\partial Y}} \tag{20}$$

$$\frac{1}{Pe} \nabla^2 \bar{T}_1 = \overline{U_1' \frac{\partial T_1'}{\partial X}} + \overline{V_1' \frac{\partial T_1'}{\partial Y}} + \bar{V}_1 \tag{21}$$

Since ϵA is considered to be smaller than unity, the oscillatory flow is dominant over the mean flowfield according to Eq. (13) so that the former is studied first. Analytical solutions to Eqs. (14-16) are difficult to obtain. Since Re is large, the inviscid solution to Eqs. (14-16) may give us some important information on the velocity field. Introducing the stream function ψ_1' such that $U_1' = \partial\psi_1'/\partial Y$, $V_1' = -\partial\psi_1'/\partial X$ and setting $F(\tau) = \cos\tau$, the inviscid solution is given as

$$\psi_1' = A_r^2 \Psi(X,Y) \sin\tau \tag{22}$$

where

$$\Psi(X,Y) = 1/2X(1/8 - X) - \frac{4}{\pi^3} \sum_{n=0}^{\infty} \left\{ \frac{(-1)^n \cos((2n+1)\pi(X-1/2)) \cosh((2n+1)\pi(Y-1/2)/Ar)}{(2n+1)^3 \cosh((2n+1)\pi/2/Ar)} \right\}$$

According to Eq. (22) ψ_1' is characterized by $\Psi(X,Y)$ spacewise, and by $\sin\tau$ timewise. The function Ψ is plotted in Fig. 3 for $Ar = 1$. As seen in the figure, the fluid motion is unicellular spacewise.

To obtain the complete solutions, the set of Eqs. (14-21) were solved numerically. Since they are linear systems, the numerical procedures are simpler than those required to solve the complete equations (9-12). Equations (14-16) were solved first. The latter equations were put into the form of vorticity equation, which was then written in a finite difference form (forward-time and centered-space approximation). Since the vorticity equation is linear, the finite difference equations were quite adequately solved by the standard ADI method.[8] After U_1' and V_1' were computed at each time step, T_1' was computed using the same method. As for the mean flowfield, its driving forces are given by the time averaged inertia, convection, and body force terms associated with the fluctuating flowfield. To compare the driving forces terms such as $U_1' \partial U_1'/\partial X$ are approximated by $U_{1,i}'(U_{1,i+1}' - U_{1,i-1}')/(2\Delta X)$, and their time average values were computed after each cycle. After about 3 to 4 cycles those averages were found to become independent of the integration time. Once the driving forces were determined, the mean velocity and

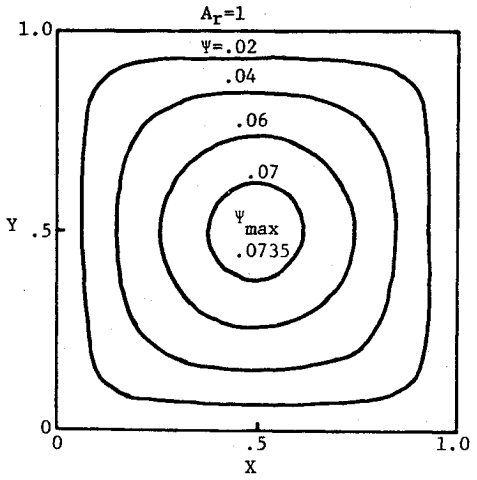

Fig. 3 Distribution of inviscid function Ψ.

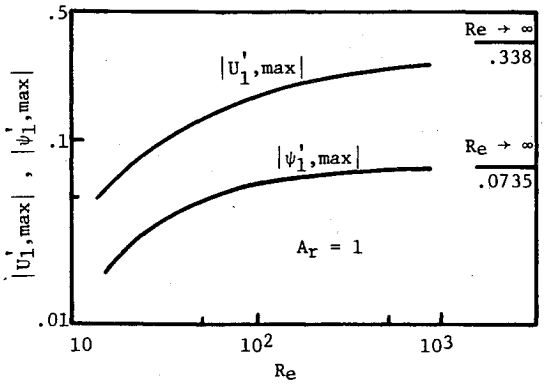

Fig. 4 Velocity oscillation level for $Ar=1$.

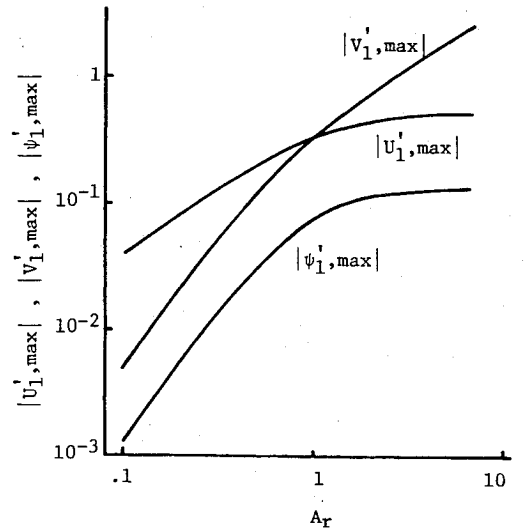

Fig. 5 Inviscid velocity oscillation levels as function of Ar.

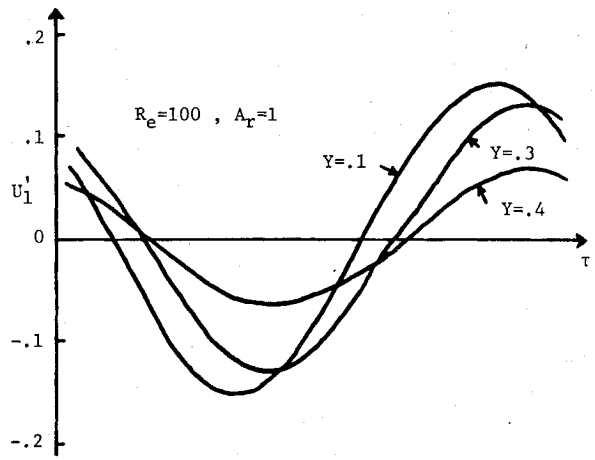

Fig. 6 Phase shifts in velocity oscillations.

temperature fields were computed using the successive over-relaxation method. The problem was studied in the ranges $Re \leq 1000$, $0.01 \leq Pr \leq 10$ and $Ar=1$. $F(\tau)$ was taken as $\cos\tau$. After some computation at 11×11 grid system for $Re \leq 200$ and 16×16 for $Re>200$ were found to be adequate. As for the time step size 32 steps per cycle were found to give stable solutions for all the ranges of the parameters studied herein. Using the numerical results several aspects of the problem are discussed below. The magnitudes of the oscillatory fluid velocities U_i' and V_i', stream function ψ_i' and temperature T_i' are represented herein by the maximum values in the container, namely $|U_i'|_{max}$, $|V_i'|_{max}$, $|\psi_i'|_{max}$, and $|T_i'|_{max}$.

Figure 4 shows the values of $|U_i'|_{max}$ and $|\psi_i'|_{max}$ for various values of Re and $Ar=1$. Both increase with Re, and approach those for the above inviscid solution. Beyond $Re=1000$ those values do not change appreciably. Figure 5 shows the values of $|U_i'|_{max}$, $|V_i'|_{max}$ for various values of Ar calculated from the inviscid solution. All the values increase with Ar.

One important effect of viscosity is that it gives rise to phase shifts in the velocity oscillations. Figure 6 shows the velocity changes with time at different Y locations at $X=0.5$. As seen in the figure the fluid particles at different Y locations are not oscillating synchronously. The phase shift becomes more noticeable towards the wall.

The temperature distribution depends on Pr as well as Re. Figure 7 shows the values of $|T_i'|_{max}$ for various values of Pr and Re. As seen in Eq. (17) when Pe is very large, $|T| \simeq |V|$. According to Fig. 7 that happens in the region $Pe \geq 500$ for $Ar=1$. Below $Pe=500$ the temperature fluctuation level becomes smaller as Pr decreases for a given value of Re.

As explained above if $\epsilon < \epsilon A \ll 1$ or if the reduced gravity level is important, there are corrections to the above velocity field. Those corrections result in the mean velocity field. The mean flowfield is discussed using the numerical results. If the reduced gravity level F_m is on the order of 10^{-7}-10^{-9} g_0, $a\omega^2$ 10^{-3}-10^{-4} g_0 and ϵA about 0.1, then $(1/\epsilon A)F_m/a\omega^2 < 10^{-2}$ so that the term was considered to be negligible in the numerical analysis. According to Eq. (19) the mean flowfield is caused by the inertia terms of the fluctuating-velocity field and by the body force associated with the fluctuating-temperature field. As discussed above when Pr is much less than unity, the temperature oscillation is much smaller than the velocity oscillation so that in that case the mean flowfield is mainly caused by the inertia terms. This kind of mean fluid motion is generally called streaming motion.[9] A typical streaming motion in the present problem is presented in Fig. 8, where $\bar{\psi}_1$ is defined such that $\bar{U}_1 = \partial\bar{\psi}_1/\partial Y$, $\bar{V}_1 = -\partial\bar{\psi}_1/\partial X$. The flow pattern is such that the fluid is pushed out from the corners along the walls, and for $Ar=1$, as seen in Fig. 8, a pair of counter-rotating eddies in one quadrant are symmetric. For later use we denote $\bar{\psi}_{1,1}$ and $\bar{\psi}_{1,2}$ for the values of $\bar{\psi}_1$ at the center of the eddies (Fig. 8). As Pr becomes large the temperature oscillations become important. It was found that as Pr increases the mean flowfield changes in such a way that the value of $\bar{\psi}_{1,1}$ becomes larger than $\bar{\psi}_{1,2}$, and eventually the eddies associated with $\bar{\psi}_{1,2}$ disappear. A typical example is shown in Fig. 9. The values of $\bar{\psi}_{1,1}$ and $\bar{\psi}_{1,2}$ for various values of Re and Pr are plotted in Fig. 10. For $Pr=0.01$ the asymmetry appears around $Re=300$, and for $Pr=1$ $\bar{\psi}_{1,2}$ disappears around $Re=100$.

As for the mean temperature field the ratio of $\bar{T}_1$ to T_0 is $(\epsilon A)^2$ so that $\bar{T}_1$ has to be very large to modify T_0 and thus to

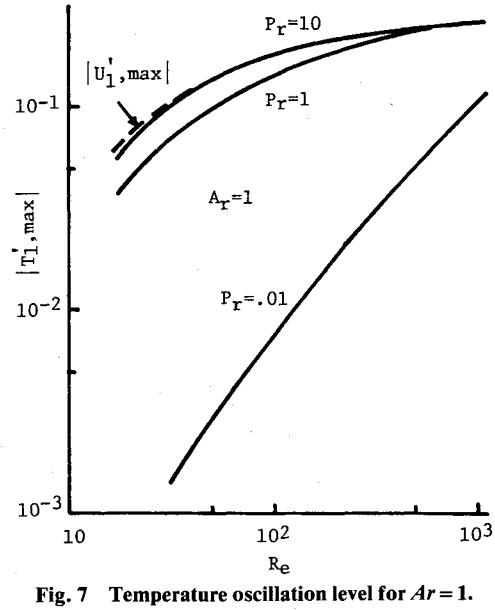

Fig. 7 Temperature oscillation level for $Ar = 1$.

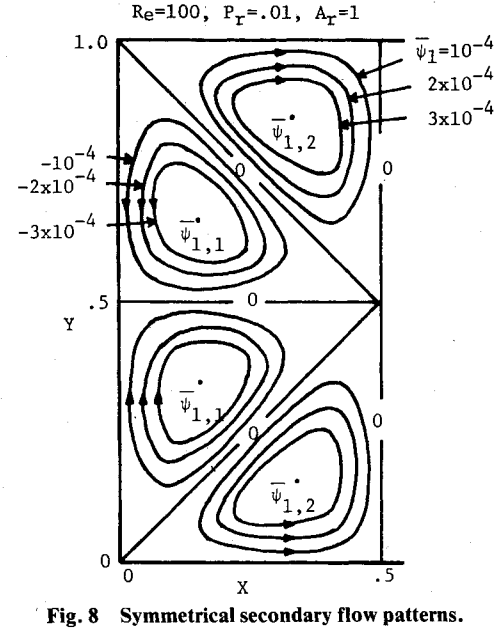

Fig. 8 Symmetrical secondary flow patterns.

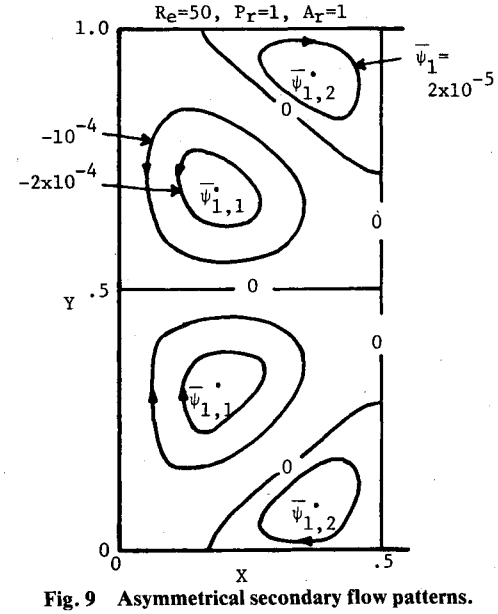

Fig. 9 Asymmetrical secondary flow patterns.

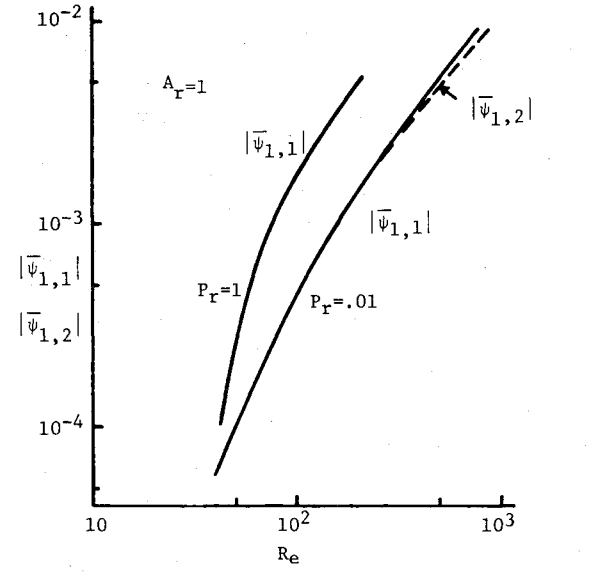

Fig. 10 Magnitude of secondary flow.

change the heat transfer rates at the walls. An inspection of Eq. (21) reveals that the value of $\bar{T}_1$ increases with Pr and Re. According to the present numerical calculations the heat transfer rate changes only about 2% from that of conduction at $Pr = 1$ and $Re = 500$. Therefore for the ranges of the parameters studied herein the effect of $\bar{T}_1$ on T_0 is considered to be very small.

Other Aspects of the Problem

In the above analysis both the temperature distribution (T_0) and g jitter (f_x) were assumed to be in steady states. The situations where either one is in a transient state are discussed below.

In the case where the heating starts at $t = 0$ we set $T_0 = 0$ everywhere for $t < 0$, and $T_0 = 1$ at $Y = 1$ for $t \geq 0$. Then the solution to Eq. (8) using t instead of τ is given as

$$T_0 = \sum_{n=0}^{\infty} \operatorname{erfc} \frac{2n+1-Y}{2\sqrt{\alpha t/L_y}} - \sum_{n=0}^{\infty} \operatorname{erfc} \frac{2n+1+Y}{2\sqrt{\alpha t/L_y}} \qquad (23)$$

where α is thermal diffusivity and $\alpha t/L_y^2$ is dimensionless temperature diffusion time. Figure 11 shows the changes of $|U_1,\max|$, $|T_1,\max|$ and $|\psi_1,\max|$ with time as T_0 develops. The profiles of T_0 at several times are also shown. As seen in the figure, the stream function increases monotonically with time, indicating that the flow as a whole increases its strength with time. The changes of U_1 and T_1 with time indicate that locally the velocity and temperature oscillation levels go slightly above the steady-state levels. The same trends were found for other values of Pr and Re.

Another transient case is when T_0 is steady but f_x starts at $t = 0$. An accurate treatment of this case is rather complex because in general f_x does not necessarily start as a well defined sinusoidal function. The profiles of f_x during the adjustment period depend on how the external forces are applied to the spacecraft. However, barring some large peaks in f_x during the period, the velocity and temperature oscillation levels are expected to be of the same orders as those for the steady state.

Another aspect of the problem is the effect of the g-jitter acting parallel to the imposed temperature gradient. Suppose f_y is expressed as $f_y = a_y \omega^2 F(\tau)$ (both ω and $F(\tau)$ are considered to be approximately the same as those for f_x), then eliminating the pressure terms from Eqs. (10) and (11), the body force term in the resulting vorticity equation is given as

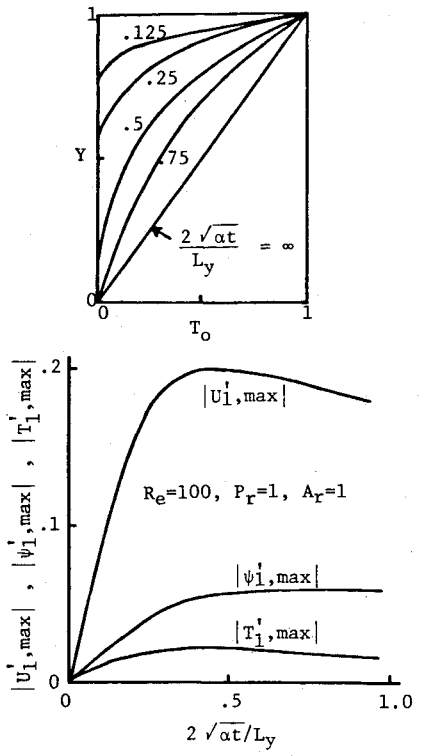

Fig. 11 Velocity and temperature oscillation levels during transient period.

(F_m is considered to be negligible as before)

$$A_r^2\left[\frac{\partial T_0}{\partial Y} + \epsilon A\frac{\partial T_1}{\partial Y} - \epsilon\frac{a_y}{L_y}\frac{\partial T_1}{\partial X}\right]F(\tau)$$

The last term in the parentheses is the contribution from the parallel component. As in the case of $\epsilon a/L_x$, $\epsilon a_y/L_y$ is in general considered to be much less than unity. Therefore, the main-body force is still $\partial T_0/\partial Y F(\tau)$, that is, the oscillatory field is unaffected by the parallel component. On the other hand the mean flowfield is affected by it unless the ratio $a_y L_y/aL_x$ is small.

Probably a more important effect of the parallel component is that it may cause a thermally unstable condition (due to heating from below). Although the critical condition for the onset of thermal instability is known for constant gravity, the critical conditions for oscillatory body forces have not been studied except for the work by Gresho and Sani,[10] in which they studied the critical conditions for constant gravity superimposed by a small oscillatory body-force field. The results of the work are not applicable to the present work in which the g-jitter is assumed to be predominantly oscillatory. The stability aspect is left for future work.

Implications for Materials Processing in Space

Although the effects of the g-jitter on materials processing in space depend on the specific nature of the process, some general implications are discussed below.

It is important to note that thermal convection in an enclosure associated with spacecraft vibration is predominantly oscillatory. The magnitude of fluid particle displacement is ϵa and thus $\epsilon a/L_x$ is the magnitude relative to the dimension of the container. Since in general $\epsilon a/L_x$ is much less than unity, the fluid particles oscillate in a relatively small region. This and the fact that for materials processing the orders of Pr and Schmidt number are less than ten result in the situation where heat and mass transfer are predominantly governed by conduction and diffusion, respectively, as explained in the previous section. One thing which may be important in materials processing is the temperature oscillation in the container. The order of temperature oscillation is $\epsilon A\Delta T$ or relative to the imposed temperature difference is ϵA. Although this value is small, it may influence the dynamics of the growth front. The same is true for concentration oscillations if impurities are present.

Conclusions

The effects of g-jitter on laminar fluid motions in an enclosure whose two opposing walls are at unequal temperatures were investigated. The following conclusions are drawn from the present work.

1) The important dimensionless parameters in the problem are Re, Pr, Ar, ϵA, and $Fm/a\omega^2$. The first-order oscillatory velocity and temperature fields are characterized by Re, Pr, and Ar. The parameters ϵA and $Fm/a\omega^2$ are generally much less than unity, and their effects appear in the second- and higher-order solutions.

2) The component of g-jitter normal to the imposed temperature gradient is most important in generating thermal convection. It produces a unicellular oscillatory fluid motion. The oscillatory velocity level increases with Re for given Ar, and is of the order of $\epsilon a\omega$. The temperature oscillation level increases with Re and Pr, and is of the order of $\epsilon A\Delta T$.

3) If $\epsilon < \epsilon A \ll 1$, the oscillatory g-jitter generates a mean secondary flow which is superposed on the oscillatory flow. The secondary flow velocity is of the order of $\epsilon^2 Aa\omega$.

4) The g-jitter component parallel to the imposed temperature gradient does not cause appreciable changes in the oscillatory flowfield except possibly when the fluid becomes thermally unstable.

Acknowledgment

The financial support for this work was provided by NASA Lewis Research Center (NSG 3053).

References

[1] Grodzka, R. G., Fan, C., and Hedden, R. O., "The APOLLO 14 Heat Flow and Convection Demonstration Experiments, Final Results of Data Analyses," NASA TM X71-10901, 1971.

[2] Bannister, T. C., Grodzka, P. G., Spradley, L. W., Bourgeois, S. V., Hedden, R. O., and Facemire, B. R., "APOLLO 17 Heat Flow and Convection Experiments, Final Data Analyses Results," NASA TM X-64772, 1973.

[3] Spradley, L. W., Bourgeois, S. W., and Lin, F. N., "Space Processing Convection Evaluation, G-Jitter Convection of Confined Fluids in Low Gravity," AIAA Paper 75-695, 1975.

[4] Forbes, R. E., "The Effect of Vibration on Natural Convective Heat Transfer in a Rectangular Enclosure," Ph.D. Thesis, State College, Mississippi, 1968.

[5] Prasad, A. and Ostrach, S., "Convection Induced by G-Jitter in Rectangular Enclosure Aboard Spacecraft," Ph.D. Thesis, Rept. FTAS/TR-78-138, Case Western Reserve University, 1978.

[6] Fichtl, G. H. and Holland, R. L., "Simplified Model of Statistically Stationary Spacecraft Rotation and Associated Induced Gravity Environments," NASA TM-78164, 1978.

[7] Ostrach, S., "Laminar Flows with Body Forces," Sec. F, *High Speed Aerodynamics and Jet Propulsion*, Vol. IV, Princeton University Press, 1964.

[8] Roache, P. J., *Computational Fluid Dynamics*, Hermosa Publishers, 1972.

[9] Schlichting, H., *Boundary Layer Theory*, McGraw Hill Book Co., New York, 1960.

[10] Gresko, P. M. and Sani, R. L., "The Effects of Gravity Modulation on the Stability of a Heated Fluid Layer," *Journal of Fluid Mechanics*, Vol. 40, Part 4, 1970, pp. 783-806.